

Nuclear Shape Dynamics at Different Energy Scales

N. Minkov

Institute of Nuclear Research and Nuclear Energy,
Bulgarian Academy of Sciences, Tzarigrad Road 72, BG-1784 Sofia, Bulgaria

Received 31 October 2017

Abstract. We present a model scheme for description of odd-mass nuclei based on the consideration of quadrupole-octupole vibration-rotation motion in the even-even core and reflection-asymmetric axially-deformed motion for the odd-nucleon motion. Having incorporated fully microscopically determined K -mixing and decoupling effects due to the Coriolis interaction between the nucleon and the core, the model allows otherwise forbidden electromagnetic transitions between states built on different intrinsic configurations. We demonstrate the application of the model to the nucleus ^{229}Th showing that together with the overall quadrupole-octupole structure of the spectrum the theory is capable to explain the presence of the extremely low-energy isomer at 7.8 eV as well as to predict its γ -decay. This result suggests that the fine interplay between the collective and single-nucleon motions may govern dynamical effects in a wide range of excitations between the nuclear and atomic energy scales.

PACS codes: 21.60.Ev, 21.10.Re, 21.60.Cs, 27.90.+b

1 Introduction

The understanding of the mechanism which governs quadrupole-octupole (reflection-asymmetric) shape deformations in atomic nuclei and the explanation of variety of related effects in the structure of nuclear energy spectra and electromagnetic transitions are among the continuously challenging problems in the nuclear structure both from experimental and model points of view [1] (and references therein). The most recent experiments reconfirm the presence of stable octupole deformation in the ground states of the nuclei ^{224}Ra [2] and $^{144,146}\text{Ba}$ [3] thus underpinning the present efforts to understand the structure and dynamic properties of nuclei under the condition of complex quadrupole-octupole deformations. The problem becomes even more challenging when referred to the interplay between collective and intrinsic degrees of freedom especially important in odd mass nuclei. This was the subject of a model development involving the consideration of quadrupole-octupole vibration-rotation motion in the even-even core [4, 5], the motion of the odd nucleon within a reflection-asymmetric

axially-deformed potential [6] with BCS pairing implemented as in [7] and the Coriolis interaction between the core and the nucleon taken into account through perturbation theory in a fully microscopic way [8]. It has been shown that within this formalism the spectra of odd-mass nuclei with quadrupole-octupole degrees of freedom can be described in terms of yrast and non-yrast parity quasi-doublets (quadrupole-octupole vibration-rotation modes) built on one-quasiparticle excitations (bandheads) mixed through the Coriolis coupling [8]. It was demonstrated for the spectra of ^{223}Ra and ^{221}Fr that the model reasonably takes into account both the Coriolis K -mixing and decoupling effects and thus appears capable to reproduce the fine structure of quadrupole-octupole spectra in odd-mass nuclei.

Recently the model was applied to the low-lying spectrum of ^{229}Th with a focus on the extremely low-energy isomeric state of 7.8 eV with $K^\pi = 3/2^+$. By taking into account the Coriolis K -mixing effect we were able to predict non-zero values for the reduced $B(E2)$ and $B(M1)$ probabilities for a transition of this state to the ground state with $K^\pi = 5/2^+$ [9]. Apart from the circumstance that this prediction is of a special interest for experimentalists who aim to observe such transitions the obtained result gives an indication that the fine interplay between collective and single-nucleon degrees of freedom may govern not only dynamical properties at the typical nuclear energy scale but could also be responsible for the presence of effects manifesting at the scale between nuclear and atomic physics. Then a natural question arising in this respect is whether and to what extent nuclear structure model could provide any reliable estimation at such a low-energy scale? As mentioned in Ref. [9] one way to clarify this question is to examine the model description at different physical conditions imposed on the solution of the problem. The purpose of the present work is to examine in more details a solution obtained at a different condition for the collective quadrupole-octupole vibration mode. More precisely we consider oscillation quantum numbers which differ from those assumed in [9] and try to clarify how this affects the model predictions for the both overall structure of the spectrum and the particular characteristics of the $K^\pi = 3/2^+$ isomeric state including its E2 and M1 decay modes.

In Section 2 we present the model formalism, while in Section 3 the particular result for ^{229}Th is given together with a relevant discussion. In Section 4 concluding remarks are given.

2 Model of Quadrupole-Octupole (QO) Core Plus Particle

The Hamiltonian of QO vibrations and rotations coupled to the s.p. motion with Coriolis interaction and pairing correlations can be written in the form

$$H = H_{\text{s.p.}} + H_{\text{pair}} + H_{\text{qo}} + H_{\text{Coriol}}. \quad (1)$$

Here $H_{\text{s.p.}}$ is the single-particle (s.p.) Hamiltonian of Deformed Shell Model (DSM) with the Woods-Saxon (WS) potential for axial quadrupole, octupole

and higher multipolarity deformations [6] providing the s.p. energies E_{sp}^K with given value of the projection K of the total and s.p. angular momentum operators \hat{I} and \hat{j} , respectively on the intrinsic symmetry axis. H_{pair} is the standard BCS pairing Hamiltonian [10] which together with $H_{\text{s.p.}}$ determines the quasi-particle (q.p.) spectrum ϵ_{qp}^K as shown in Ref. [7]. H_{qo} represents oscillations of the even-even core with respect to the quadrupole (β_2) and octupole (β_3) axial deformation variables mixed through a centrifugal (rotation-vibration) interaction [5]. Its spectrum is obtained in an analytic form by assuming equal frequencies for the quadrupole and octupole oscillations known as coherent QO mode (CQOM). H_{Coriol} involves the Coriolis interaction between the even-even core and the unpaired nucleon (see Eq. (3) in [5](a)). It is treated as a perturbation with respect to the remaining part of Hamiltonian (1) and then incorporated into the QO potential of H_{qo} defined for given angular momentum I , parity π and s.p. band-head projection K_b which leads to a joint term [8]

$$H_{\text{qo}}^{IK_b} = -\frac{\hbar^2}{2B_2} \frac{\partial^2}{\partial \beta_2^2} - \frac{\hbar^2}{2B_3} \frac{\partial^2}{\partial \beta_3^2} + \frac{1}{2} C_2 \beta_2^2 + \frac{1}{2} C_3 \beta_3^2 + \frac{\tilde{X}(I^\pi, K_b)}{d_2 \beta_2^2 + d_3 \beta_3^2}. \quad (2)$$

Here, B_2 (B_3), C_2 (C_3) and d_2 (d_3) are quadrupole (octupole) mass, stiffness and inertia parameters, respectively. The function $\tilde{X}(I^\pi, K_b)$ determines the centrifugal term in which the Coriolis mixing is taken into account and has the form:

$$\tilde{X}(I^\pi, K_b) = \frac{1}{2} \left[d_0 + I(I+1) - K_b^2 + (-1)^{I+\frac{1}{2}} \left(I + \frac{1}{2} \right) a_{\frac{1}{2}}^{(\pi\pi^b)} \delta_{K_b, \frac{1}{2}} \right. \\ \left. - A \sum_{\substack{\nu \neq b \\ (K_\nu = \frac{1}{2}, K_b \pm 1)}} \frac{\left[\tilde{a}_{K_\nu K_b}^{(\pi\pi^b)}(I) \right]^2}{\epsilon_{\text{qp}}^{K_\nu} - \epsilon_{\text{qp}}^{K_b}} \right], \quad (3)$$

where d_0 determines the QO potential origin, the quantity $a_{1/2}^{(\pi, \pi^b)} = \pi \pi_b a_{\frac{1}{2} - \frac{1}{2}}^{(\pi^b)}$ represents the decoupling factor for the case $K_b = 1/2$ and $\tilde{a}_{K_\nu K_b}^{(\pi, \pi^b)}$ represent the Coriolis mixing factors:

$$\tilde{a}_{K_\nu K_b}^{(\pi, \pi^b)}(I) = \begin{cases} \sqrt{(I - K_b)(I + K_b + 1)} a_{K_\nu K_b}^{(\pi^b)}, & K_\nu = K_b + 1, \\ \sqrt{(I + K_b)(I - K_b + 1)} a_{K_b K_\nu}^{(\pi^b)}, & K_\nu = K_b - 1, \\ \pi \cdot \pi^b (-1)^{(I+\frac{1}{2})} (I + \frac{1}{2}) a_{\frac{1}{2}, -\frac{1}{2}}^{(\pi^b)}, & K_\nu = K_b = \frac{1}{2}, \end{cases} \quad (4)$$

with

$$a_{K_\nu K_b}^{(\pi^b)} = \frac{P_{K_\nu K_b}^b}{N_{K_\nu}^{(\pi^b)} N_{K_b}^{(\pi^b)}} \langle \mathcal{F}_{K_\nu}^{(\pi^b)} | \hat{j}_+ | \mathcal{F}_{K_b}^{(\pi^b)} \rangle = \frac{P_{K_b K_\nu}^b}{N_{K_b}^{(\pi^b)} N_{K_\nu}^{(\pi^b)}} \langle \mathcal{F}_{K_b}^{(\pi^b)} | \hat{j}_- | \mathcal{F}_{K_\nu}^{(\pi^b)} \rangle. \quad (5)$$

Nuclear Shape Dynamics at Different Energy Scales

The latter involve matrix elements of the s.p. operators $\hat{j}_\pm = \hat{j}_x \pm i\hat{j}_y$ between the parity-projected components of the s.p. wave functions $\mathcal{F}_{K_b}^{(\pi^b)}$ of the band-head state and the admixing state $\mathcal{F}_{K_\nu}^{(\pi^b)}$ determined by DSM [6]. Each s.p. wave function, which has a mixed parity due to the reflection asymmetry, is projected on the experimentally assigned good parity π^b of the band-head s.p. state. The quantity $N_K^{(\pi^b)} = \left[\langle \mathcal{F}_K^{(\pi^b)} | \mathcal{F}_K^{(\pi^b)} \rangle \right]^{\frac{1}{2}}$ is a parity-projected normalization factor, whereas $P_{K_\nu', K_\nu}^b = U_{K_\nu'}^b U_{K_\nu}^b + V_{K_\nu'}^b V_{K_\nu}^b$ involves the BCS occupation factors. The index b corresponds to the blocked s.p. orbital on which the collective spectrum is built. Since the BCS procedure is performed separately for each band-head orbital (blocked) the overlap integrals and the matrix elements between states built on different band-head orbitals involve the average of both separate occupation factors $P_{K_\nu', K_\nu}^{bb'} = \frac{1}{2} \left(P_{K_\nu', K_\nu}^b + P_{K_\nu', K_\nu'}^{b'} \right)$. The sum in (3) runs over q.p. states with energies $\epsilon_{qp}^{K_\nu}$ above the Fermi level and A is the Coriolis mixing strength defined in [8]. In our numerical calculations we consider ten mixing orbitals.

In this consideration the spectrum which corresponds to Hamiltonian (1) represents QO vibrations and rotations built on a q.p. state with $K = K_b$ and parity π^b . The corresponding energy expression has the form [8]

$$E_{nk}^{\text{tot}}(I^\pi, K_b) = \epsilon_{qp}^{K_b} + \hbar\omega \left[2n + 1 + \sqrt{k^2 + b\tilde{X}(I^\pi, K_b)} \right], \quad (6)$$

where $b = 2B/(\hbar^2 d)$ denotes the reduced inertia parameter and $n = 0, 1, 2, \dots$ and $k = 1, 2, 3, \dots$ stand for the radial and angular QO oscillation quantum numbers, respectively, with k odd (even) for the even (odd) parity states of the core [4]. The levels of the total QO core plus particle system, determined by a particular n and $k^{(+)}$ ($k^{(-)}$) for the states with given $I^{\pi=+}$ ($I^{\pi=-}$) form a split doublet with respect to the parity, called *quasi parity-doublet* (QPD) [5](b). Furthermore, $\omega = \sqrt{C_2/B_2} = \sqrt{C_3/B_3} \equiv \sqrt{C/B}$ stands for the frequency of the coherent QO oscillations and $d = (d_2 + d_3)/2$ [4, 5].

The Coriolis perturbed wave function corresponding to Hamiltonian (1) with the spectrum (6) is obtained in the first order of perturbation theory and has the form

$$\tilde{\Psi}_{nkIMK_b}^{\pi, \pi^b} = \frac{1}{\tilde{N}_{I\pi K_b}} \left[\Psi_{nkIMK_b}^{\pi, \pi^b} + A \sum_{\substack{\nu \neq b \\ (K_\nu = K_b \pm 1, \frac{1}{2})}} C_{K_\nu K_b}^{I\pi} \Psi_{nkIMK_\nu}^{\pi, \pi^b} \right], \quad (7)$$

where the expansion coefficients are given by $C_{K_\nu K_b}^{I\pi} = \tilde{a}_{K_\nu K_b}^{(\pi \pi^b)}(I) / (\epsilon_{qp}^{K_\nu} - \epsilon_{qp}^{K_b})$ and $\tilde{N}_{I\pi K_b}^2 = \langle \tilde{\Psi}_{nkIMK_b}^{\pi, \pi^b} | \tilde{\Psi}_{nkIMK_b}^{\pi, \pi^b} \rangle$ is the normalization constant of the form

N. Minkov

$$\begin{aligned}
\tilde{N}_{I\pi K_b}^2 &= 1 + 2A \sum_{\substack{\nu \neq b \\ (K_\nu = K_b = \frac{1}{2})}} C_{K_\nu K_b}^{I\pi} \delta_{K_\nu K_b} \frac{P_{K_\nu K_b}^b}{N_{K_\nu}^{(\pi^b)} N_{K_b}^{(\pi^b)}} \langle \mathcal{F}_{K_\nu}^{(\pi^b)} | \mathcal{F}_{K_b}^{(\pi^b)} \rangle \\
&+ A^2 \sum_{\substack{\nu_1 \neq b \\ (K_{\nu_1} = K_b \pm 1, \frac{1}{2})}} \sum_{\substack{\nu_2 \neq b \\ (K_{\nu_2} = K_b \pm 1, \frac{1}{2})}} C_{K_{\nu_1} K_b}^{I\pi} C_{K_{\nu_2} K_b}^{I\pi} \delta_{K_{\nu_1} K_{\nu_2}} \\
&\quad \times \frac{P_{K_{\nu_1} K_{\nu_2}}^b}{N_{K_{\nu_1}}^{(\pi^b)} N_{K_{\nu_2}}^{(\pi^b)}} \langle \mathcal{F}_{K_{\nu_1}}^{(\pi^b)} | \mathcal{F}_{K_{\nu_2}}^{(\pi^b)} \rangle. \quad (8)
\end{aligned}$$

The unperturbed QO core plus particle wave function in Eq. (7) has the form [8]

$$\begin{aligned}
\Psi_{nkIMK}^{\pi, \pi^b}(\eta, \phi, \theta) &= \frac{1}{N_K^{(\pi^b)}} \sqrt{\frac{2I+1}{16\pi^2}} \Phi_{nkI}^{\pi, \pi^b}(\eta, \phi) \\
&\quad \times \left[D_{MK}^I(\theta) \mathcal{F}_K^{(\pi^b)} + \pi \cdot \pi^b (-1)^{I+K} D_{M-K}^I(\theta) \mathcal{F}_{-K}^{(\pi^b)} \right], \quad (9)
\end{aligned}$$

where $D_{MK}^I(\theta)$ are the rotation (Wigner) functions and $\Phi_{nkI}^{\pi, \pi^b}(\eta, \phi)$ are the QO vibration functions obtained after solving the Schrödinger equation for the Hamiltonian (2) in radial (η) and angular (ϕ) coordinates (see [4, 5] for details).

Having the Coriolis perturbed wave function (7) and using the theory for electric transition probabilities in CQOM developed in [4](b) we were able to calculate the reduced probabilities $B(E1)$, $B(E2)$ and $B(E3)$ for transitions between initial (i) and final (f) states with energies given by Eq. (6). Also, by using the standard form of the M1 operator given in Ref. [10] [e.g. see Eq. (3.61) therein] we have obtained an expression for the respective $B(M1)$ transition probability. It appears that the expressions for both types (T), electric ($T = E$) and magnetic ($T = M$) transition with multipolarity λ can be derived in a common form

$$\begin{aligned}
B(T\lambda; \pi^{b_i} I_i \pi_i K_i \rightarrow \pi^{b_f} I_f \pi_f K_f) &= R^{T\lambda} \delta_{\pi^{b_f} \pi^{b_i}} [(1 + \pi_f \pi_i (-1)^{\lambda \delta_{T,E}}) / 2] \\
&\quad \times \frac{1}{\tilde{N}_{I_f \pi_f K_f}^2 \tilde{N}_{I_i \pi_i K_i}^2} \left[\delta_{K_f K_i} C_{I_i K_i \lambda 0}^{I_f K_f} \frac{P_{K_f K_i}^{b_f b_i} M_{K_f K_i}^{\pi^{b_f} \pi^{b_i}}}{N_{K_f}^{(\pi^{b_f})} N_{K_i}^{(\pi^{b_i})}} \right. \\
&\quad + AC_{I_i K_f \lambda 0}^{I_f K_f} \sum_{\substack{\nu \neq i \\ (K_\nu = K_i \pm 1, \frac{1}{2})}} \delta_{K_f K_\nu} C_{K_\nu K_i}^{I_i \pi_i} \frac{P_{K_f K_\nu}^{b_f} M_{K_f K_\nu}^{\pi^{b_f} \pi^{b_i}}}{N_{K_f}^{(\pi^{b_f})} N_{K_\nu}^{(\pi^{b_i})}} \\
&\quad \left. + AC_{I_i K_i \lambda 0}^{I_f K_i} \sum_{\substack{\nu \neq f \\ (K_\nu = K_f \pm 1, \frac{1}{2})}} \delta_{K_\nu K_i} C_{K_\nu K_f}^{I_f \pi_f} \frac{P_{K_\nu K_i}^{b_i} M_{K_\nu K_i}^{\pi^{b_f} \pi^{b_i}}}{N_{K_\nu}^{(\pi^{b_f})} N_{K_i}^{(\pi^{b_i})}} + \right.
\end{aligned}$$

Nuclear Shape Dynamics at Different Energy Scales

$$\begin{aligned}
 & + A^2 \sum_{\substack{\nu'' \neq f \\ (K_{\nu''} = K_f \pm 1, \frac{1}{2})}} \sum_{\substack{\nu' \neq i \\ (K_{\nu'} = K_i \pm 1, \frac{1}{2})}} \delta_{K_{\nu''} K_{\nu'}} C_{I_i K_{\nu'} \lambda K_{\nu''} - K_{\nu'}}^{I_f K_{\nu''}} \\
 & \times C_{K_{\nu''} K_f}^{I_f \pi_f} C_{K_{\nu'} K_i}^{I_i \pi_i} \left[\frac{P_{K_{\nu''} K_{\nu'}}^{b_f b_i} M_{K_{\nu''} K_{\nu'}}^{\pi_f \pi_i}}{N_{K_{\nu''}}^{(\pi_f)} N_{K_{\nu'}}^{(\pi_i)}} \right]^2, \quad (10)
 \end{aligned}$$

where

$$R^{T\lambda=E\lambda} = \frac{2\lambda + 1}{4\pi(4 - 3\delta_{\lambda,1})} R_\lambda^2(\pi^{b_i} n_i k_i I_i \rightarrow \pi^{b_f} n_f k_f I_f) \quad (11)$$

involves integrals on the radial and angular variables in CQOM [see Eqs. (35)–(41) and Appendices B and C in Ref. [4](b)] and

$$R^{T1=M1} = \frac{3}{4\pi} \mu_N^2 \quad (12)$$

involves the nuclear magneton. Also here

$$M_{K_f K_i}^{\pi_f \pi_i} = \begin{cases} \langle \mathcal{F}_{K_f}^{(\pi_f)} | \mathcal{F}_{K_i}^{(\pi_i)} \rangle, & \text{for } T = E \\ \left[(g_l - g_R) K_i \delta_{K_f K_i} \langle \mathcal{F}_{K_f}^{(\pi_f)} | \mathcal{F}_{K_i}^{(\pi_i)} \rangle \right. \\ \left. + (g_s - g_l) \langle \mathcal{F}_{K_f}^{(\pi_f)} | \hat{s}_z | \mathcal{F}_{K_i}^{(\pi_i)} \rangle \right], & \text{for } T = M, \end{cases} \quad (13)$$

where $g_R = Z/A_{\text{mass}}$ is the rotation gyromagnetic factor, \hat{s}_z is the z -component of the spin operator, $g_l = 0$ (1) for neutrons (protons) is the orbital gyromagnetic factor, whereas the spin gyromagnetic factor is $g_s = 0.6 g_s^{\text{free}}$ with $g_s^{\text{free}} = -3.826$ (5.586) for neutrons (protons). The symbol $C_{I_1 K_1 \lambda \mu}^{I_2 K_2}$ denotes the Clebsch-Gordan coefficient.

We note that the reduced transition probability expression (10) contains first-order and second-order K -mixing effects. First-order mixing terms practically contribute with nonzero values only in the cases $K_{i/f} = K_\nu = 1/2$, i.e., when a $K_{i/f} = 1/2$ bandhead state is mixed with another $K_\nu = 1/2$ state present in the considered range of admixing orbitals above the Fermi level. A second-order mixing effect connects states with $\Delta K = 1, 2$ and allows different combinations of $|K_i - K_f| \leq 2$ which provide respective nonzero contribution of the Coriolis mixing to the transition probability. In this way the present formalism provides nonzero transition probabilities between states with different K -values despite the axial symmetry assumed in both CQOM and DSM parts of Hamiltonian (1).

3 The QPD Spectrum and Extremely Low-Energy Isomer in ^{229}Th

Here we illustrate the application of the above core plus particle scheme on the QPD spectrum of the nucleus ^{229}Th . We apply the algorithm as explained on

page 3 of Ref. [9]. Thus, we consider that the low-lying spectrum of this nucleus represents an yrast (yr) QPD built on the $K_{b\text{yr}}^\pi = 5/2^+$ ground state corresponding to the $5/2[633]$ s.p. orbital and a non-yrast [excited (ex)] QPD built on the isomeric $K_{b\text{ex}}^\pi = 3/2^+$ state corresponding to the $3/2[631]$ s.p. orbital with both quasi-doublets having the same value $n = 0$ of the radial quadrupole-octupole oscillation quantum number. In Ref. [9] we have also supposed that the pairs of angular quantum numbers for the positive and negative-parity counterparts in the two quasi-doublets are identical, namely $k_{\text{yr}}^{(+)} = k_{\text{ex}}^{(+)} = 1$ and $k_{\text{yr}}^{(-)} = k_{\text{ex}}^{(-)} = 2$. However now we consider that the k^- values of the both doublets can differ from 2 and in addition can differ from one another. In this work we study in more details the case of $k_{\text{yr}}^{(-)} = 6$ and $k_{\text{ex}}^{(-)} = 8$. As mentioned in [9] this is among the model conditions which provide better overall description of the low-lying spectrum in ^{229}Th including the $3/2^+$ isomeric state. The remaining calculation conditions including quadrupole-octupole deformation parameters and pairing constants in the deformed shell model are the same as explained in [9].

In Figure 1 we present the model description obtained in this particular case. We see that the theory (left part) reproduces the overall QPD structure of the experimental (right) spectrum. The root mean square (rms) deviation of the

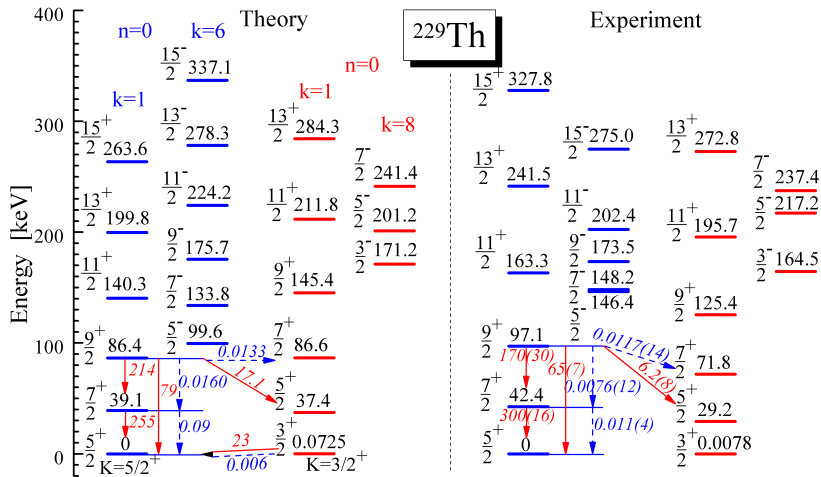


Figure 1. (color online) Theoretical and experimental QPD levels of ^{229}Th in the case of angular quantum numbers $k_{\text{yr}}^{(-)} = 6$ and $k_{\text{ex}}^{(-)} = 8$ with $k_{\text{yr/ex}}^{(+)} = 1$. Theoretical and experimental values for B(E2) (in red) and B(M1) (in blue-dash) reduced transition probabilities are also given. The B(E2) and B(M1) values for the $3/2^+_{\text{ex}} \rightarrow 5/2^+_{\text{yr}}$ transition are predicted. The CQOM model parameters used are $\omega = 0.06 \text{ MeV}/\hbar$, $b = 4.5 \hbar^{-2}$, $d_0 = 45 \hbar^2$, $c = 320$, $p = 1$ and $A = 0.144 \text{ keV}$. The experimental data are taken from Ref. [11] for the energies and Ref. [12] for the available transition probabilities.

Nuclear Shape Dynamics at Different Energy Scales

predicted energy levels from the experimental ones is $\text{rms}_{\text{yr}} = 36.4$ keV for the yrast-based band and $\text{rms}_{\text{ex}} = 12.4$ keV for the isomer-based band, with the total deviation being $\text{rms}_{\text{tot}} = 27.8$ keV.

As a result of the overall fit the theoretical $3/2^+$ isomer energy is obtained at 0.0725 keV. Though this value is about an order of magnitude larger than the experimental one from nuclear structure point of view the result looks reasonable. Actually, from Ref. [9] it is known that we can exactly fit the experimental value by a very fine tuning of the CQOM parameters. This is achieved on the expense of a slight deterioration (increase) of the overall rms factor by up to 1 keV. Since in the present case the obtained theoretical value is closer to the experimental one compared to the value in Figure 1 of [9] we may expect that the corresponding deterioration will be smaller. On the other hand it is also known that such a refinement does not change essentially the predicted values of decay probabilities [9]. This means that from nuclear structure point of view the result obtained in the overall fit corresponds to the natural capability of the model to gain an insight into the considered isomer phenomenon in the energy scale close to the border of atomic physics phenomena.

In addition to the energy levels in Figure 1 we give the theoretical $B(E2)$ and $B(M1)$ values for several electric and magnetic transitions compared with the respective experimental data given also there. It is seen that the agreement between the theoretical and experimental transition values for the available data is quite good. We also remark that in the presently considered case of $k_{\text{yr}}^{(-)} = 6$ and $k_{\text{ex}}^{(-)} = 8$ this agreement is even better compared to the case of $k_{\text{yr/ex}}^{(-)} = 2$ in [9]. Also we remark that the overall agreement in the energy description here is better than the one in Figure 1 of [9] where $\text{rms}_{\text{tot}} = 34$ keV and $\text{rms}_{\text{ex}} = 26$ keV. Here the rms factor for the isomer-based band is smaller by a factor of two.

On the top of the above observations we remark that the present case suggests a bit smaller values for the predicted $B(E2)$ and $B(M1)$ transition probabilities for the $3/2^+$ isomer decay compared to those in [9], with $B(E2) = 22.86$ W.u. and $B(M1) = 0.0063$ W.u., respectively. Actually, in [9] these values are considered to be close to the lower border of the estimated intervals of predicted transition probabilities, $B(E2)=20-30$ W.u. and $B(M1)=0.006-0.008$ W.u.

In this way the present result illustrates the stability of the model predictions for the $3/2^+$ radiative decay made in [9]. At the same time it points out that it is possible to search for various ways to improve the overall model description of the ^{229}Th spectrum including the $3/2^+$ isomeric state on a purely nuclear model level. It is, therefore, believed that any further refinement or clarification of the fine structure effects which determine the energy and the transition properties of this nucleus in relation to its 7.8 eV isomer would be of a special use for experimental studies from the both nuclear and atomic physics points of view.

4 Concluding Remarks

In conclusion, we remark that the consistent model consideration of the complex shape dynamics and the single-nucleon motion allows us to identify and/or take into account certain specific effects of the fine interplay between different degrees of freedom on the structure of energy spectra and the attendant electromagnetic rates in odd-mass nuclei. The considered case of ^{229}Th suggests that the underlying dynamical mechanism may govern the manifestation of collective and intrinsic nuclear properties in a wide range of energies from the typical nuclear scale to the tiny scale towards the border with atomic physics. Therefore, it is interesting to see if similar behavior and analogical effects could be identified in other nuclei in the same region or elsewhere in the nuclear chart. The study in this direction could be a subject of further work.

Acknowledgement

This work has been supported by the Bulgarian National Science Fund under contract No. DFNI-E02/6.

References

- [1] P.A. Butler and W. Nazarewicz (1996) *Rev. Mod. Phys.* **68** 349.
- [2] L.P. Gaffney et al. (2013) *Nature (London)* **497** 199; P.A. Butler (2016) *J. Phys. G: Nucl. Part. Phys.* **43** 073002.
- [3] B. Bucher et al. (2016) *Phys. Rev. Lett.* **116** 112503; (2017) *Phys. Rev. Lett.* **118** 152504.
- [4] (a) N. Minkov, P. Yotov, S. Drenska, W. Scheid, D. Bonatsos, D. Lenis and D. Petrellis (2006) *Phys. Rev. C* **73** 044315; (b) N. Minkov, S. Drenska, M. Strecker, W. Scheid and H. Lenske (2012) *Phys. Rev. C* **85** 034306.
- [5] (a) N. Minkov, S. Drenska, P. Yotov, S. Lalkovski, D. Bonatsos and W. Scheid (2007) *Phys. Rev. C* **76** 034324; (b) N. Minkov, S. Drenska, K. Drumev, M. Strecker, H. Lenske and W. Scheid (2013) *Phys. Rev. C* **88** 064310.
- [6] S. Cwiok, J. Dudek, W. Nazarewicz, J. Skalski and T. Werner (1987) *Comp. Phys. Comm.* **46** 379.
- [7] P.M. Walker and N. Minkov (2010) *Phys. Lett. B* **694** 119.
- [8] N. Minkov (2013) *Phys. Scripta* **T154** 014017.
- [9] N. Minkov and A. Pálffy (2017) *Phys. Rev. Lett.* **118** 212501.
- [10] P. Ring and P. Schuck (1980) *The Nuclear Many-Body Problem* (Heidelberg: Springer).
- [11] <http://www.nndc.bnl.gov/ensdf/>.
- [12] http://www.nndc.bnl.gov/nudat2/indx_adopted.jsp.